12

Distributed Smart Sensing Systems for Indoor Monitoring of Respiratory Distress Triggering Factors

Octavian Postolache, José Miguel Pereira,
Pedro Silva Girão and Gabriela Postolache
Instituto de Telecomunicações ESTSetubal (LabIM),
Polytechnic Institute of Setúbal Escola de Saúde,
Universidade Atlântica
Portugal

1. Introduction

Indoor air quality pollution [1][2] represents one of the factors associated with the etiology of chronic obstructive pulmonary disease and also plays an important role in respiratory distress, the second most common symptom of adults that request emergency transportation to the hospital and is associated with a relatively high overall mortality before hospital discharge [3][4][5][6]. The prevention of acute respiratory distress or asthma attacks can be possible by monitoring the air quality conditions using distributed smart sensing systems characterized by accuracy, short time response, and robustness as well as by data processing, data logging and data communication capabilities.

Considering the importance of indoor air quality monitoring, different distributed measuring system architectures and associated calibration methods and systems are presented in the literature [7][8][9]. The main elements of these kind of systems are not only temperature and relative humidity sensors, but also gas detectors and gas concentration sensors whose metrological characteristics, such as accuracy and linearity are very limited, which implies the design and implementation of signal processing algorithms namely for numerical linearization and common factors correction [10][11][12].

Taking into account the indoor spatial distribution of the temperature and relative humidity values as well as the concentration values of pollutants (e.g CO, CO_2 resulting of combustion), the development of distributed measuring systems [13][14] that can include personal computers (PCs) or mobile devices (e.g. PDAs [15] or smart phones [16]) based human-sensing system interface represents an important requirement for optimal indoor air quality monitoring.

This chapter presents a practical approach concerning distributed smart sensing solutions for air quality monitoring, highlighting the original contributions of the authors in this area. The first part of the chapter deals with the relation between the subject's health status, respiratory distress condition and air quality conditions. The second part contains a brief presentation of solid state sensors [17] that materialize the sensing component of air quality monitoring systems and the third part presents a distributed architecture based on an

embedded Web server for air quality monitoring including elements of data processing. In the fourth part, a Bluetooth wireless distributed system including smart sensing nodes and a smart phone programmed as assisted human - distributed air quality monitoring system interfacing device is presented.

Referring to the distributed air quality monitoring system based on embedded Web server nodes, the sensing part of each node is expressed by a thick film metal oxide semi-conductor sensor array that includes general air contaminant, alcohol and organic solvent detection, and CO sensing. The measurement data and pollution alarms from the nodes, which are parts of a wired or wireless network, are obtained through the browser that accesses the nodes' Web pages. A set of temperature and relative humidity sensors are included in the node's hardware in order to increase the gas sensor accuracy through the correction of temperature and humidity influences. This chapter also includes a brief description of the multiple-input–single-output neural network design and implementation [18] that is used to obtain temperature and humidity compensated gas concentration values on the client software side. A Bluetooth enabled wireless sensing network designed and implemented for continuous monitoring of indoor humidity and temperature conditions as well as to detect general air contaminants is described in the chapter. Bluetooth compatible nodes, characterized by data acquisition capabilities, are connected to a mobile device expressed by a smart phone programmed using Java2ME to perform different tasks including data communication, data logging, data processing, alarm generation and graphical user interfacing with the indoor air quality monitoring system. Elements regarding the smart phone embedded software configuration and logged data transfer according to the network architecture and air quality monitoring tasks are discussed and an example of particular implementation is also presented. Using the distributed measurement system, an intelligent assessment of air conditions for risk factor reduction of asthma or chronic obstructive pulmonary disease is proposed.

2. Air quality and its impact on respiratory diseases

Air conditions and respiratory assessment represent an important challenge taking into account that distress is the second most common symptom of adults transported by ambulance and is associated with a relatively high overall mortality before hospital discharge [3]. Among the most common causes of respiratory distress in this setting are congestive heart failure, pneumonia, chronic obstructive pulmonary disease and asthma [4]. It is projected that chronic obstructive pulmonary disease (COPD) will be the third leading cause of death worldwide by 2020, due to an increase in smoking rates and demographic changes in many countries [5]. Worldwide, some 300 million people currently suffer from asthma. It is the most common chronic disease among children [6]. The economic burden of COPD in the US in 2007 was 42.6 billion in health care costs and lost productivity [19]. The indoor air pollution is one of the factors associated with etiology of chronic obstructive pulmonary disease and asthma. There are evidences that the environmental factors acting during early life and interacting with specific "asthma genes" are crucial for the development of chronic, persistent form of disease [20][21]. The identification of the indoor air associated with pathophysiology of COPD and asthma disease will thus be crucial for the primary-prevention strategy.

Poor indoor air quality is becoming an increasing problem around the world because, in general, people are spending more time indoors. This problem is greater in infants who now

spend less time playing outside. Reduction of indoor air quality - produced by mould growth, smoke exposure, cooking fire smoke (often using biomass fuels such as wood and animal dung), house dust mites in bedding, carpets and stuffed furniture, chemical irritants (i.e. perfumes), pet dander – may adversely affect the health of building occupants and exacerbate asthma and COPD attacks. Asthma attacks are mainly related to mould growth that is enabled by relative humidity high values for different temperature conditions. Mould spores, bacteria, and mildew thrive in dampened towels, washcloths, and moist or humid areas. Additionally, people with immune or respiratory system problems may more easily succumb to poor health caused by mould growth at home, which is mainly associated with humidity and temperature values. Improved heating systems and less ventilation from outside has also provided more suitable conditions for mould growth. Using air conditions sensing components as parts of an air quality measuring system, high risk disease conditions for indoor occupants can be avoided. Several solutions have been presented in the literature [9][13][22]. In order to assure mobility and flexibility, a wireless network for air quality is an interesting solution considering that the measuring nodes can be distributed in different regions of the house according with different monitoring scenarios. As the interface between a user and the network (human machine interface, HMI), can be used a low cost smart phone (Bluetooth enabled), a PDA (personal digital assistant), or situated displays with interaction capabilities (touch screen enabled).

3. Air quality sensing and data processing

This section contains the description of the main components of a distributed smart sensing system that can be used for air quality assessment. Particular attention is dedicated to the implementation of the sensing nodes, to signal conditioning, and to signal processing of measurement data.

A. Sensing nodes

The sensing nodes are designed and implemented to perform the air quality (AirQ) monitoring using low cost gas sensors and, at the same time, to get additional information about the temperature (T) and relative humidity (RH). This information is used to increase gas concentration measurement accuracy, performing the error compensation caused by temperature and humidity influence.

The gas sensors can be sintered SnO_2 semiconductor heated sensors, as those provided by Figaro [23], that assure pollution event detection (TGS800 – general air contaminant sensor - AC), methane detection (TGS842-M), alcohol and organic solvent detection (TGS822-SV) and carbon monoxide detection (TGS203-CO). Information about temperature and relative humidity are obtained using Smartec SMT160-30 [24] and Humirel HM1500 [25] temperature and relative humidity transducers, respectively.

The gas sensors, connected to proper conditioning circuits, are devices that produce voltages whose values depend on the concentrations of gas expressed in ppm. The used conditioning circuit for the air pollution sensor TGS800, solvent vapors (TGS822) and methane sensor (TGS842) are presented in figure 1.

Electrochemical cells can also be used to implement the sensing units. The NAP-505 [17] is a typical example of this kind of implementation. In this cased, the 3 terminals measuring cell consists of 3 porous noble metal electrodes separated by an acidic aqueous electrolyte,

housed within a plastic enclosure. The working principle of the sensing unit is based on chemical reactions between gas and other elements. From the electrical charges that are involved in those reactions it is possible to measure an electrical current that is proportional to gas concentration. Using multiple cells it is possible to measure the concentration of different gas types.

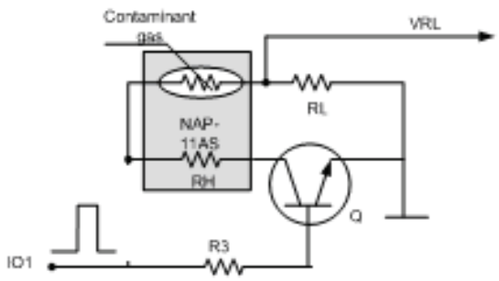

Fig. 1. Gas sensing unit based on semiconductor heated sensors (Vc – circuit voltage, VH – heater voltage, VGS – gas sensor output voltage, RL – load resistance)

Figure 2 represents the main elements of a gas sensing unit based on an electrochemical cell.

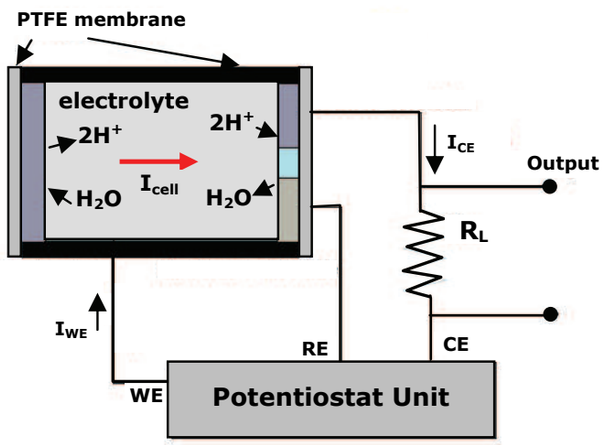

Fig. 2. Gas sensing unit based on an electrochemical cell (RE - reference electrode, CE - counting electrode, WE - working electrode, RL – load resistance)

The measuring cell includes a working electrode (WE), a counter electrode (CE) and a reference electrode (RE) [26]. The conditioning circuit is basically a potentiostat unit that measures the gas dependent current amplitude (I_{cell}) that flows between the CE and WE through cell's electrolyte. The current amplitude is directly proportional to the gas concentration but its value is usually very low, about a few tens of nA. For this reason a careful design of the potentiostat is crucial to obtain an acceptable measurement. Figure 3 represents the electrical diagram of a typical potentiostat conditioning circuit [27][28]. The negative feedback loop, provided by operational amplifiers (OA1 and OA2) and the electrical connection that exists between CE and RE electrodes through the sensing element,

assures that the operational amplifiers are working in their linear zones. Since the current between the working and the reference electrodes is very low, the differential voltage between working and counter electrodes is equal to VRE and the output voltage (VADC) from the current to voltage converter implemented by sub-circuit 2 is given by

$$V_{ADC} = -R_F \cdot \left[f_{sol.}(V_{DAC}) - I_B \right] \tag{1}$$

where RF represents the feedback resistor of the current to voltage converter, IB represents the polarization current of OA2, VDAC is the output voltage of the D/A converter and fsol is generally a non-linear function that depends on solution characteristics and applied voltage (VWE).

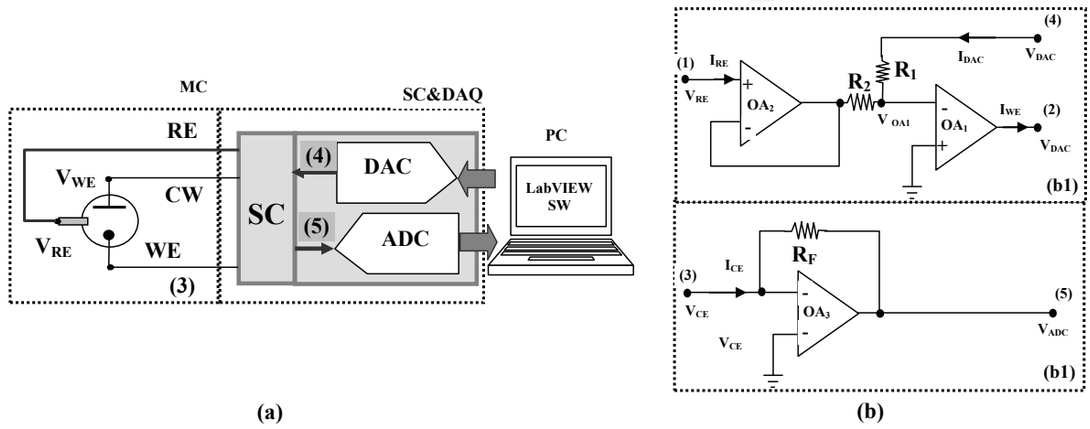

Fig. 3. Electrical circuit of a voltammetry measuring system (MS- measuring cell, RE- reference electrode, CE- counting electrode, WE- working electrode, SC&DAQ- signal conditioning and data acquisition, ADC- analogue to digital converter, DAC- digital to analog converter, OA- operational amplifier)

Another attractive solution that can be used to implement the sensing nodes is based on surface acoustic wave (SAW) devices [29][30]. The sensor consists of an interdigitated transducer etched onto a piezoelectric substrate, covered with a thin film. The mass of the film increases as its material selectively adsorbs a chemical substance from the air. This causes a shift in resonance to a slightly lower frequency giving information about the amount of gas species in the air.

B. Measurement data interpolation

To perform the interpolation of the calibration data in order to obtain the inverse characteristic of the measurement data, two methods are usually considered, namely, polynomial interpolation and artificial neural networks (ANNs).
Assuming, for simplicity, a single variable function (f) and a LMS polynomial interpolation function defined by [31]

$$P_n(x) = \sum_{k=0}^{p} \alpha_k \cdot x^k \tag{2}$$

where *p* represents the degree of the polynomial curve fitting function and *x* represents the independent variable - measured quantity - it is possible to demonstrate that the LMS deviation between calibration and curve fitting data is obtained when the coefficients of the curve fitting polynomial function are given by

$$[\alpha] = \left[X_C^T \cdot X_C\right]^{-1} \cdot \left[X_C^T \cdot Y\right] \tag{3}$$

being vector Y and matrix X_C defined, for a set or n calibration points, by

$$Y = \begin{bmatrix} y_1 \\ y_2 \\ : \\ y_n \end{bmatrix} \quad X_C = \begin{bmatrix} 1 & x_1 & x_1^2 & \cdots x_1^p \\ 1 & x_2 & x_2^2 & \cdots x_2^p \\ : & : & : & \cdots : \\ 1 & x_n & x_n^2 & \cdots x_n^p \end{bmatrix} \tag{4}$$

The concerns related with polynomial interpolation are mainly associated with the choice of the polynomial degree. If a low polynomial degree is used, the interpolation error is generally high because the polynomial function can not fit correctly a large number of calibration points. Conversely, if an excessive polynomial degree is used, the LMS deviation between calibration data and the values obtained from the polynomial interpolation function may be very low, but the interpolation errors of points between calibration data are usually very high. This problem is usually known as overfitting and the previous one as underfitting.

Regarding ANN [18][32][33], the curve fitting function can be computed using the following expression:

$$F_{ANN}(x_i) = F_N\left(W_N * \left(F_{N-1}\left(\ldots F_2\left(W_2 * F_1(W_1 * x_i + B_1) + B_2\right)\ldots + B_{N-1}\right) + B_N\right)\right. \tag{5}$$

where N represents the number of neural network (NN) layers, Bi the bias vectors, Wi the weight vectors and Fi the activation transfer function of each layer.

The most common ANN structure for measurement applications contains a hidden layer of neurons with sigmoidal activation functions whose input is the measured data, and an output layer of neurons with linear activation functions. This ANN structure calculates an output vector given by

$$F_{ANN}(x_i) = \text{purelin}\left(W_2 * \text{tansig}(W_1 * x_i + B_1) + B_2\right) \tag{6}$$

where purelin() and tansig() are linear and hyperbolic tangent sigmoidal activation transfer functions, respectively.

This architecture has proved capable of approximating any function with a finite number of discontinuities and with arbitrary accuracy. Generally a more complex function, such as transducer characteristics that are strongly non-linear, requires more sigmoidal neurons in the hidden layer.

To evaluate the capability of a given solution to generalize the learned function, a second more dense set of data points - testing set - is used and the correspondent interpolated errors are evaluated. The best values of [B] and [W] matrices, associated with the bias and weights of each neuron, can be computed by minimizing the mean square error

$$MSE(x) = \frac{1}{n}\sum_{i=1}^{n}\left(F_{ANN}(x_i) - y_i\right)^2 \tag{7}$$

Several gradient methods [34][35], like back propagation (generalized Δ rule), can minimize the error function during the ANN training phase. During training, a set of input values corresponding to the calibration points is used to adjust the weights and biases of the neurons by minimizing the difference between the ANN output and the calibration values.
Even if there is no general rule to choose polynomial or ANN based curve fitting methods for a given application, when a reduced number of calibration points are available, and especially when extrapolation capabilities are desired, ANN can usually give better results in terms of measurement accuracy. This is particularly true for non-linear and non-deterministic sensors' characteristics and, if the number of calibration points is small, there is not an excessive penalty in terms of the computational load caused by an higher number of mathematical operations, usually caused by the need to evaluate non-linear transfer functions (tanh()) [36][37][38][39].

C. Data processing: an application example

In order to take advantage of the joint use of polynomial and artificial neural network (ANN) curve fitting techniques [12][40], this section describes a hybrid solution based on polynomial modelling (PM) and artificial neural networks modelling (ANN-M) that can be used to estimate the values of air quality parameters, such as, temperature, relative humidity, and polluting gases concentration.
For the particular case of broadband gas sensors, different methods can be used to convert the measured data into concentration of possible gas contaminants, such as, methane, carbon monoxide, isobutane, hydrogen, ethanol or cigarette smoke. Considering the voltage generated by a gas sensing unit based on a semiconductor heated sensor (TGS800 from Figaro), an air quality index ζ, is defined using the following relation

$$\zeta = \frac{R_S}{R_{S0}} = \left(\frac{V_C}{V_{RL}} - 1\right) \cdot \frac{1}{\left(\frac{V_C}{V_{RL0}} - 1\right)} \tag{8}$$

where R_{S0} represents the sensor resistance for a clean air condition, R_S represents the sensor resistance for the tested air, V_C is the circuit power supply voltage, V_{RL} is the load resistor voltage and V_{RL0} is the load resistor voltage for clean air.
Sensor's characteristic is non-linear and monotonic, decreasing sensor's resistance ratio with contaminant gas concentration. Higher concentrations of contaminants originate lower values of resistance ratios. Moreover, since the sensor is designed for general contaminants detection, it is not possible to identify specific contaminants. So, according to the application requirements in terms of the maximum acceptable level of contamination, a coefficient (ζ) value equal to 0.3 is considered for air pollution alarm. Considering that the used sensor has not good selectivity for each potential air contaminant, a look-up table, a polynomial, and a multilayer perceptron single-input single output neural network were designed and implemented to convert the value of ζ into air contaminants' concentrations expressed in parts per million (ppm). The measurement data processing scheme that was implemented is represented in figure 4.

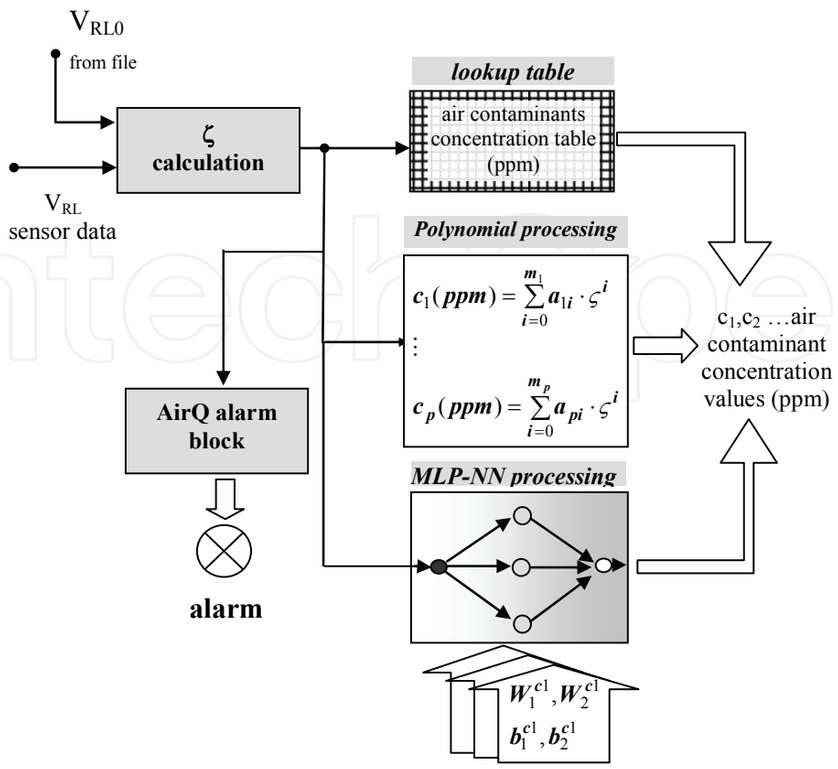

Fig. 4. Block diagram of the hybrid data processing scheme that was used to evaluate contaminants' air concentrations.

To test the performance of the proposed modeling scheme, a set of coefficient values (ζ), contained in the interval between 0.15 and 1 (no pollution), and the correspondent values of air contaminants' concentrations obtained from TGS800 sensitivity curves for methane, carbon monoxide, isobutane, hydrogen and ethanol, were considered. The calculation of polynomial coefficients, a_{1i}, a_{2i}, … a_{pi}, is based on LS linear fit function (Givens method) that is implemented in LabVIEW. The calculated polynomial coefficients values that correspond to TGS800 sensitivity curves, such as the ones represented in figure 5, are stored in a memory and then used to perform the evaluation of air contaminants' concentrations.

The used neural processing blocks (NPB_i) is related with the inverse modeling [41] of gas sensor multivariable nonlinear characteristics, which are strongly dependent on temperature and humidity but also influenced by the concentration of other gases of the analyzed gas mixture. Based on the designed NPB_i, a digital read-out of the gases concentration with temperature and compensation [16] is obtained.

Regarding the NPB_i, two inputs one output multilayer perceptron neural networks were considered. Figure 6 represents the NPBi architecture including the normalization blocks and denormalization blocks used for ANN input and output data, respectively.

The NPB_i's internal parameters (weights and biases) are off-line calculated using the MATLAB program. The neural network training data were obtained in the system calibration phase. They are voltage values (V_{GSi}) acquired from the gas concentration measurement channel for different values of the gas concentration (C_{Gi}), and different temperature (T_p) and relative humidities (RH_i) values.

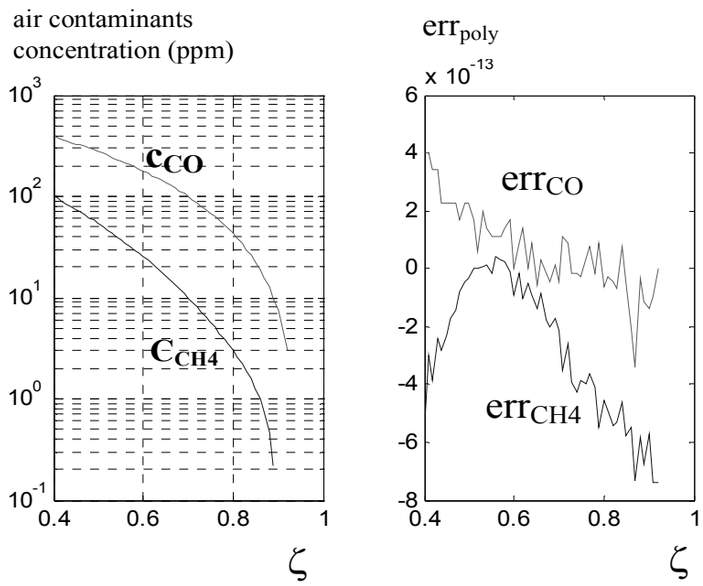

Fig. 5. Polynomial approximation of air contaminants curves (CO and methane case) and polynomial approximation error (err_{CO}, err_{CH4})

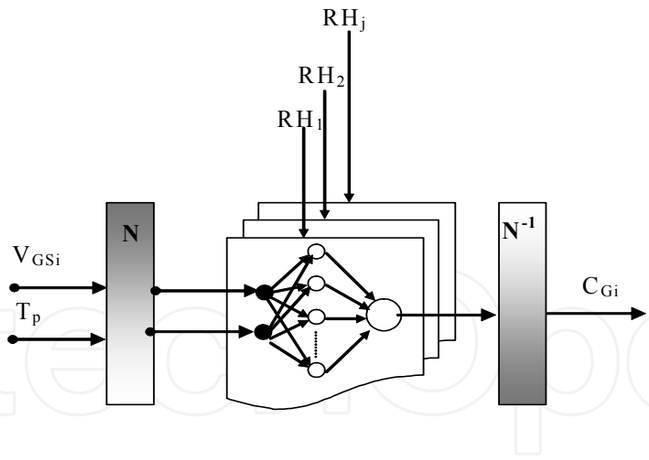

Fig. 6. NPB_i architecture (N, N^{-1}: normalization and denormalization blocks; RH_j: humidity selector; C_{Gi}: temperature and humidity compensated values of G_i gas concentration; T_P: temperature input value, V_{GSi}: input voltage value on the GS_i channel).

The neural network algorithm developed in MATLAB software calculates different sets of weights and biases for each RH_i experimental value (e.g. RH={45%, 55%, 65%}. The NPB_i input is the normalized voltage associated with each gas sensor's channel and normalized temperature, while the NPBi's output is the temperature compensated gas concentration (C_{Gi}). The NPBi normalized inputs are defined by:

$$V_{GSi}^{N}=\frac{V_{GS_i}}{V1_S},\qquad T^{N}=\frac{T}{\max(T)} \tag{9}$$

where $V1_S$ represents the gas sensor normalization factor (GS_i voltage supply=+10V in the present case).
Because GSi characteristics depend on humidity, an accurate measurement of the gas concentration is provided using different $NPB_i|_{RH}$ whose weights and biases are calculated using the data obtained for predefined relative humidity conditions (RH=45%, 55% and 65%) and by the interpolation method presented in [42].
The number of NPBi's layers is three. The hidden layers have 2 to 5 tansignoid (tansig(x)) neurons, and the output layer has 1 linear (l(x)) neuron. The implemented tansig(x) calculates its output according to

$$\text{tansig}(x)=\frac{2}{1+\exp(-2x)}-1 \tag{10}$$

which leads to a reduction of the computational load.
Two criteria for NPBi design were considered, the type and the number of neurons on the hidden layer, both determining the capabilities of the NPBi to adapt to a given characteristic. Different neuron nonlinear activation functions require different memory space and processing capabilities from the hardware platform.
To reduce the weights and biases in vector sizes, several simulation tests concerning the number of neurons for a required NPB_i performance, expressed by a modeling error, were performed. ANNs with a higher number of neurons increase processing load and, moreover, require larger memories to store weights and biases matrices. The results of these simulations are particularly important when embedded systems are used to implement the neural processing architecture (e.g. 512k EEPROM in the IPμ8930 case).
For the particular case of the CO measuring channel, the training set includes, as target, fifteen CO concentration values uniformly distributed in the 30 to 300ppm interval. The input values are the voltage values acquired from the TGS203 CO concentration measuring channel corresponding to the above-mentioned concentrations. The measured temperature in the testing chamber was T_p[°C]=10×p, p={1,2,3,4,5} and the relative humidity RH=35%. The Levenberg Marquardt algorithm [43] was used to calculate the weights and biases (W_{NPBi}, B_{NPBi}) of the neural network. Imposing a sum square error stop condition SSE=0.01, and for neural networks characterized by 4, 5 or 6 hidden neurons, different measuring channel modeling error characteristics (e_{CGsi}) were obtained (figure 7). The modeling error is defined by:

$$e_{CGsi}=\frac{C_{CGsi}-C_{CGsi}^{NPB}}{FS}\times 100 \tag{11}$$

where FS represents the measurement range, CCGsi is the experimental used gas concentration (e.g. carbon monoxide concentration) expressed in ppm, and C_{CGsi}^{NPB} the concentration of gas calculated by the corresponding neural processing module.
Since the used gas sensors characteristic depends on temperature, a study related with the CO channel modeling error (e_{CO}) versus temperature was carried out (figure 8).

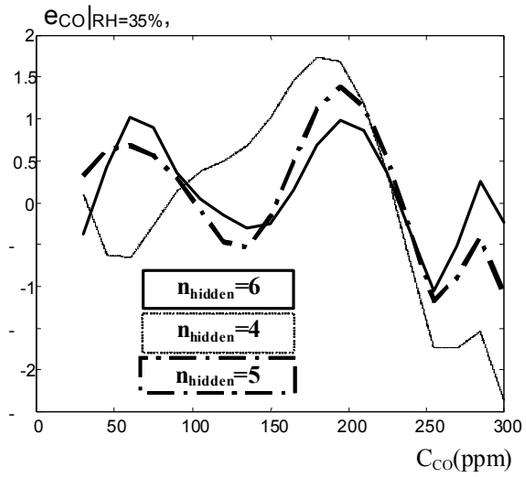

Fig. 7. The modeling error versus concentration for different NPB_{CO} architectures (T=10°C)

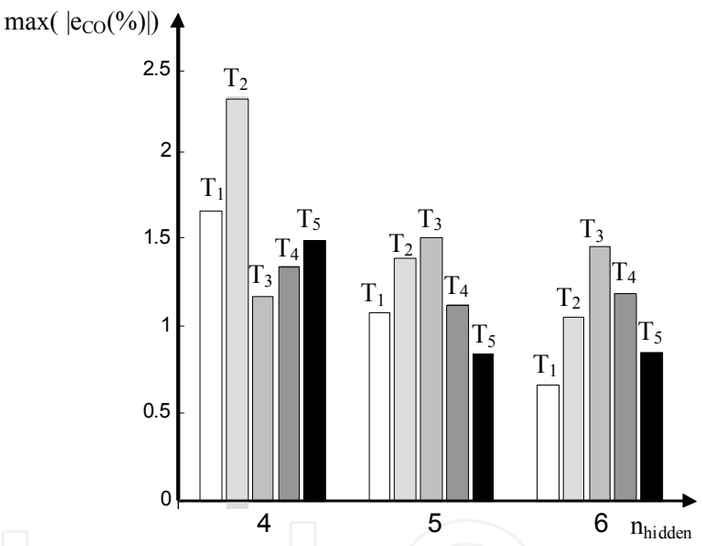

Fig. 8. The maximum inverse modeling error for different NPB_{CO} architectures (n_{hidden}={4, 5, 6}) and different temperatures T_p=10·p °C

Being humidity an influence quantity, different values of the relative humidity lead to different primary gas selectivity characteristics and hence to different gas concentration measurement accuracies. Thus, experimental data obtained for three different values of relative humidity, RH_1=35%, RH_2=65% and RH_3=95%, and five values of temperatures included in the I_T=[10;50]°C were considered. The imposed gas concentrations for measurement system testing were: 10 values of methane concentration distributed in the I_{CM}=[500;5000] ppm interval, 15 values of carbon monoxide concentration I_{CCO}=[30;300] ppm, and 15 values of solvent vapors (Ethanol vapors) concentration, C_{SV}=[50;5000] ppm.

Based on the GS_i voltages for the considered gases concentrations, and taking into account temperature and humidity, three sets of weights and biases (35%, 65% and 95% relative

humidity) were calculated for carbon monoxide, methane and solvent vapor measurement channels.

4. Smart sensing networks for air quality assessment

Gas sensors networks provide a promising mechanism for mining information from the monitored areas. Point-to-point and multipoint wireless network architectures, including sensing nodes, materialize the implementations in the air quality monitoring for indoor and outdoor conditions.

A. Point-to-point network architecture

Different architectures were developed by the authors, one of them based on a Bluetooth PDA [15]. In this case, the air quality measuring system is a virtual one (AIR-Q VMS) that joins hardware and software components to assure higher flexibility, mobility, data processing and data transmission. The block diagram of the mobile indoor air quality monitor system is presented in figure 9.

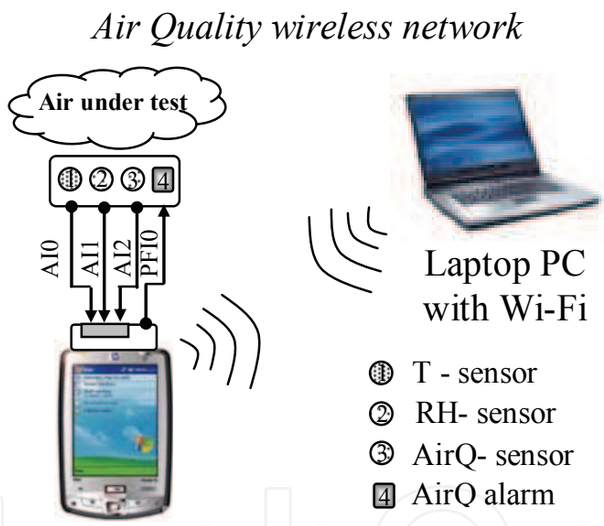

Fig. 9. Mobile Air Quality system based on a PDA with a compact flash (CF) multifunction I/O board

The sensing node includes sensors (temperature, relative humidity, and air quality), conditioning circuits, a compact flash data acquisition device DAQ (NI CF-6004) and a PDA with wireless communication capabilities (Wi-Fi or Bluetooth). A point-to-point connection between the measurement node and an advanced processing and communication unit (a PC) permits to deliver the air quality data from the sensing node to the PC and to receive information, such as alarm thresholds, that is used to implement alarm mechanisms in the PDA. The acquired data is processed by the PDA and the results are displayed by the PDA GUI.

Considering the cost of the implementation of the air quality sensing node based on a DAQ board plugged to a PDA, and also taking into account the evolution of the area of pervasive

computing,, the authors decided to develop air quality monitoring systems based on smart phones and Bluetooth enabled smart sensors. The implemented architecture is presented in figure 10.

Fig. 10. Air quality virtual measuring system's architecture based on a smart sensing node (SN) with Bluetooth communication capabilities, and on a smart phone

The smart sensors indicated in figure 10 are specialized for temperature, air quality and air quality index measurement [16]. When monitoring large spaces, the number of sensing nodes increases, which means that point-to-multipoint architectures must be considered.

B. Point-to-multipoint Bluetooth architecture and embedded smart phone software

An implementation of a point-to-multipoint network architecture that uses Bluetooth compatible smart sensing nodes is presented in figure 11. The sensing nodes provide information about the level of relative humidity, temperature, and air contaminants (e.g. undesired odours that can trigger respiratory disorders). As computation units and human machine interface are included a laptop PC that works as the system server, a touch panel computer (TPC) and a smart phone (SP).
The implemented Bluetooth scatter net architecture assures the remote monitoring of the sensing nodes and data communication between the mobile device and smart sensor nodes. The hardware component of the system includes: sensors and conditioning circuits, a data acquisition device Bluetooth enabled (e.g. BlueSentry from Grid Connect), a smart phone with Bluetooth interface (e.g. N70 from Nokia), a situated display (NI TPC2106) Bluetooth compatible through a RS232-to-Bluetooth bridge, and a data communication, data processing and data storage unit (laptop PC).

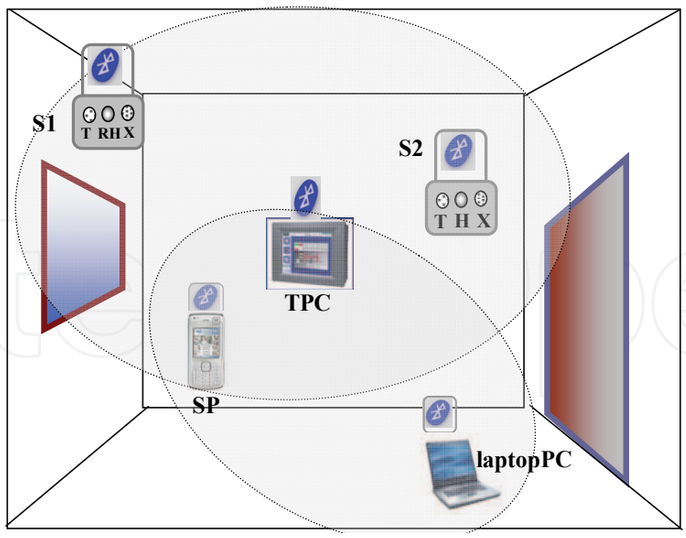

Fig. 11. Distributed air quality measurement architecture associated with respiratory distress triggering factors monitoring based on Bluetooth networking protocol (S1 and S2 are the sensing nodes characterized by T-temperature, H – relative humidity and X- air quality index measurement channel, TPC- touch panel computer, SP- smart phone)

The software technologies used to develop the applications for the smart phone running Symbian OS and for the TPC running Windows CE OS, were Java2Me and LabVIEW. The application embedded in the smart phone was named SmartSense Mobile. AirQUbicomp is the application developed using LabVIEW 8.6 Touch Panel Module for the TPC. This application provides the information about indoor air quality.

The SmartSense application has the ability to identify the active smart sensing nodes, to establish a connection via Bluetooth with the nodes, to control the on/off state of the air quality index sensor (XairQ-sensor), and to collect voltage samples from relative humidity, temperature and air quality measuring channels of each node in single-shot mode or in continuous mode.

SmartSense also assures the transfer of the indoor air quality values calculated and stored in the smart phone memory extension to the laptop PC through Bluetooth synchronization.

After node(s) selection, the operator can choose between the "one sample" acquisition and continuous acquisition. The sample acquisition is triggered by the user in order to test the normal functioning of the sensing node or to verify the measurement accuracy of the considered air parameters (humidity, temperature or broadband pollution) during the system setup.

Working in continuous acquisition mode, the smart phone application permits to prevent the asthma or COPD attacks through warnings issued when imposed thresholds previously stored in the SmartSense Mobile configuration file are exceeded. The sampling rate of the continuous acquisition mode is set using the text files received through Bluetooth from the PC that runs a SmartAdmin application [16]. Values of time intervals between two successive acquisitions in the 0.5 min to 60 min interval were considered. These values are adapted to the smart phone's available memory and also to the time constants of the system associated with temperature, humidity and XairQ index measurement. During continuous monitoring of the indoor air quality, the voltages received from the sensing nodes are

converted into physical values by the SmartSense Mobile application and stored in this format. The acquired data are saved in a file or can be sent as an SMS to the phone whose number was written in the SmartSense configuration file.
The continuous acquisition and data conversion software modules work together with an implemented alarm module that permits to generate acoustic alarms to inform that indoor air conditions are critical. The used threshold values (th) are included in table 1.

Th	Measured factors		
	RH[%]	T[°C]	XairQ[%]
thmin	30	15	50
thmax	50	30	-

Table 1. Threshold values for relative humidity, temperature and air quality index that was used to signalize a likelihood of asthma attack.

During visual or acoustic signalling, a set of useful recommendations related to indoor air factors values and the actions necessary to change the indoor air conditions from critical to normal are available through the smart phone GUI.
The AirQUbicomp application is designed to continuously monitor the air quality, generating visual and acoustic alarms according to the imposed thresholds. Active interaction with the touch panel computer is permitted after identification of the user through a numeric password. After identification, the user can modify the thresholds related to asthma or can define data logging elements such as the time between readings and the monitoring period (DLog TAB in Fig. 12). The values of temperature, air quality and air quality index as well as the alarms LEDs (AirQ Alarm) are part of the T-RH-XAirQ software TAB. In figure 12 the GUI associated with AirQUbicomp is presented.

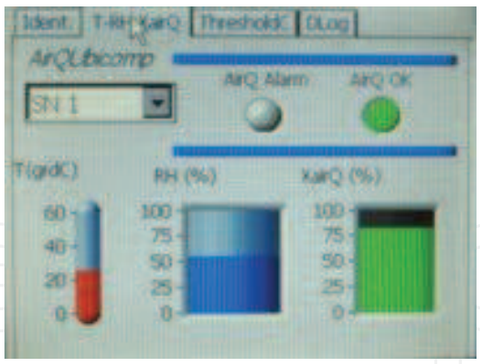

Fig. 12. AirQUbicomp GUI

Using the developed SmartSense Mobile application different tests associated with indoor air quality monitoring were carried out. The data stored in the Nokia N70, is wireless transferred to the database implemented in the laptop PC. Some data related with continuous measurement of the asthma or COPD attack triggering factors are presented in figure 13.
In figure 13 (a) the relative humidity is in the limit of automatic alarm generation (RH>50%) while temperature and air quality are inside the interval values associated with "no asthma or COPD attack conditions".

In figure 13 (b) can be observed low levels of the XairQ index when the measurement session started. Based on the information displayed, the user acted to improve the air quality (e.g. by opening the window). The air quality started to improve and, at the same time, room's temperature and humidity change significantly.

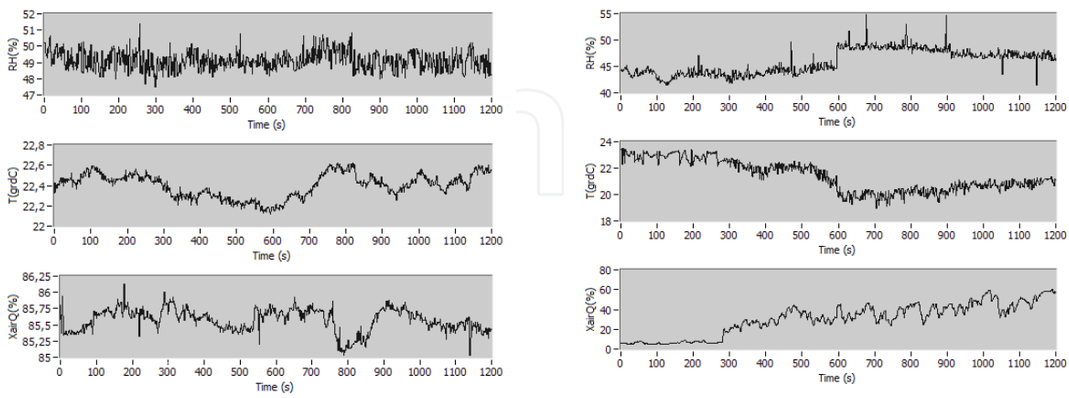

a) b)

Fig. 13. S1 node monitoring of respiratory distress triggering factors

In order to find correlations between the air quality and the values of physiological parameters, such as oxygen saturation (SpO2) and heart rate (HR), a digital pulse oxymeter and electrocardiograph apparatus ECG Medlab P-OX 100 was used for testing purposes. Table 2 presents the results of SpO2 and HR for two volunteers, with and without respiratory distress history (RD-N, RD-Y). The physiological values were measured in the same room and for the volunteers seated on a chair.
Analyzing the data from table 2, one can notice that in case of the healthy individual (RD-N), values of XairQ lower than 80% and of RH near 50% do not induce changes in HR and SpO2, while a significant increase in the HR of RD-Y is felt.

Sensor node	T (°C)	RH (%)	XairQ (%)	RD-N		RD-Y	
				HR	SpO2	HR	SpO2
S1	17.2	47.4	62.7	72	98	96	92
S2	17.8	44.2	69.6				

Table 2. S1 node: air quality and physiological parameter values for two volunteers, with and without respiratory distress history

Nowadays, smart phones are provided with operating systems, such as Android OS and iOS, which make the implementation of complex software modules easier and faster. The authors have been working to develop an AirQ Android OS application for a multichannel sensing node. The graphical interface of the implemented application is presented in figure 14.
The AirQ dashboard includes elements related with respiration activity (respiration rate). The data logging procedure is done using a smart phone embedded database that can synchronize with Web-based information system database through Wi-Fi or 3G/UMTS communication protocol.

Fig. 14. AirQ graphical interface implemented in the AndroidOS smart phone

5. Conclusion

The quality of life of pulmonary patients greatly depends on the quality of the air they breathe. The identification of the indoor air associated with pathophysiology of COPD and asthma disease is crucial for the primary-prevention strategy. In the preceding paragraphs the authors summarize the main elements of a distributed smart sensing network for indoor air quality assessment. Regarding sensing nodes and signal conditioning, two possible solutions were presented. One based on semiconductor heated sensors and another based on three electrodes' cells. For data processing purposes, a hybrid solution based on polynomial and artificial neural networks modelling is presented. The last part of the chapter includes possible solutions for indoor air quality smart sensing networks.

6. References

[1] USA Environment Protection Agency, "Indoor Air Quality", on-line at http://www.epa.gov/iaq/

[2] European Environment Agency, "Every breath you take — air quality in Europe", on-line at http://www.eea.europa.eu/articles/air-quality-in-europe

[3] I.G. Stiel, D.W. Spaite, B. Field, L.P. Nesbitt, D. Munkley, J. Maloney et al, "Advanced life support for out-of hospital respiratory distress", NEJM, vol. 356, issue 24, pp. 2156-64, 2007

[4] K.F. Rabe, S. Hurd, A. Anzuento, P.J. Barnis, S.A. Buist, P. Calverley, et al, "Global strategy for the diagnosis management, and prevention of chronic obstructive pulmonary disease: GOLD executive summary", Am J Respir Crit Care Med, vol. 176, issue 6, pp. 532-55, 2007

[5] J.C. Hogg, F. Chu, S. Utokaparch S et al, "The nature of small-airway obstruction in chronic obstructive pulmonary disease", NEJM, vol. 350, issue 26, pp. 2645-53, 2004
[6] WHO, 2007, Asthma: http://www.who.int/topics/asthma/en/2007
[7] J. Bartolomeo, "Detecting CO in the home", Home Automation and Building Control, pp. 51–55, Oct. 1995.
[8] F. Sarry and M. Lumbreras, "Gas discrimination in an air-conditioned system", IEEE Trans. Instr. Meas., vol. 49, no. 4, pp. 809–812, Aug. 2000
[9] O. Postolache, J.M. Dias Pereira, P. Girão, "Smart sensor network for air quality monitoring", Proc. IEEE Instrumentation and Measurement Technology Conf., Ottawa, Canada, vol. 1, pp. 537 - 542, 2005
[10] S. Marco, A. Ortega, A. Pardo, and J. Samitier, "Gas identification with tin oxide sensor array and self-organizing maps: Adaptive correction of sensor drifts", IEEE Trans. Instr. Meas., vol. 47, no. 1, pp. 316–320, Feb. 1998
[11] F. Ménil, M. Susbielles, H. Debéda, C. Lucat, and P. Tardy, "Evidence of a correlation between the non-linearity of chemical sensors and the asymmetry of their response and recovery curves," Sens. Actuators B, Chem., vol. 106, no. 1, pp. 407–423, Apr. 29, 2005
[12] J. M. Dias Pereira, P. M. B. Silva Girão, and O. Postolache, "Fitting transducer characteristics to measured data", IEEE Signal Process. Mag., vol. 4, no. 4, pp. 26–39, Dec. 2001
[13] N. Ulivieri, C. Distante, T. Luca, S. Rocchi, P. Siciliano, "IEEE1451.4: A way to standardize gas sensor", Sens. Actuators B: Chemical vol. 114, issue 1, pp. 141-151, 2006
[14] Octavian A. Postolache, J. M. Dias Pereira, P. M. B. Silva Girão "Smart sensors Network for Air Quality Monitoring Applications", IEEE Trans. Instr. Meas., Vol. 58, No. 9, Sept. 2009
[15] O. Postolache, P. Girão, M. Pereira, "PDA based virtual measuring system for broadband air quality monitoring", Proc. IMEKO World Congress, on CD, September, Brasil, 2006
[16] O. Postolache, P. Girão, J. M. Dias Pereira, N. Barroso, G. Ferreira, G. Postolache, "Indoor monitoring of respiratory distress triggering factors using a wireless sensing network and a smart phone", Proc. of I2MTC 2009, Singapore, May 2009
[17] Nemoto Chemical Sensors Catalogue, Nemoto & Co., Tokyo, Japan, on line at http://www.nemoto.co.jp/product
[18] S. Haykin, "Neural Networks: A Comprehensive foundation (2nd Edition)", Wiley, 1998.
[19] NHLBI Morbidity and Mortality Chart Book, on line at http://www.nhlbi.nih.gov/resources/docs/cht-book.htm
[20] C.M. Patino, F.D. Martinez, "Interaction between genes and environment in the development of asthma", Allergy, vol. 56, pp.279-86, 2001
[21] Indoor Air Quality Impacts Child Asthma, Humidex Reduces Contaminates that Trigger Asthma Attacks, on line at http://www.naturalnews.com/010255.html
[22] M. Tomizuka, C. Bang Yun, V. Giurgiutiu, "A smart indoor air quality sensor network", Proc. of SPIE, Smart Structures and Materials, vol. 6174, pp. 1277-1290, 2006
[23] Figaro, "Gas sensors catalog", on line at http://www.figaro.co.jp/en/make_html/item_1.html.

[24] Smartec, "Smartec- Sensors Catalog", on line at http://www.mmselectronics.co.uk/smt160-30.htm.
[25] Humirel, "Relative Humidity Sensor-HS1100", Humirel Inc, 1999
[26] J.M. Dias Pereira, O. Postolache, Ricardo Salgado, P. Silva Girão, "Voltammetry based automated instrument for in-situ and on-line measurement of heavy metals concentration in water", 1st IMEKO TC19 Symposium on Measurement and Instrumentation for Environmental Monitoring, pp. 85-90, Iasi, Romania, September 2007
[27] J.M. Dias Pereira, O. Postolache, P. Silva Girão, "A smart and portable solution for heavy metals concentration measurements", 24th IEEE Instrumentation and Measurement Technology Conference (IMTC/2007), Warsaw, Poland, May 2007
[28] M. D. Pereira, O. Postolache, P. S. Girão, "Improving celerity of heavy metals measurements", International Instrumentation & Measurement Technology Conference 2010 (I2MTC'2010), pp. 1073-1077, Austin, May 2010
[29] R.M. White, F.W. Voltmer, "Direct piezoelectrical coupling to surface elastic waves", Applied Physics Letters, (7), pp. 314-316, 1965
[30] S.Y. Yurish and M.T. Gomes, "Smart Sensors and MEMS", Proc. of the NATO Advanced Study Institute, II-Mathematics, Physics and Chemistry, Vol. 181, Kluwer Academic Publisher, September 2003
[31] S.D. Conte, C. de Boor, "Elementary numerical analysis: An algorithmic approach", 2nd edition, New York, McGraw-Hill, 1972
[32] H. Demuth, M. Baele, "Neural Network Toolbox for Use with MATLAB – User's Guide", The MathWorks Inc., September 1993
[33] J. Hertz, A. Krogh, R.G. Palmer, "Introduction to the theory of neural computation", Addison Wesley, 1991
[34] F. M. Silva, L. B. Almeida, "Speeding up backpropagation", Advanced Neural Computers, R. Eckmiller edition, pp. 151-160, North Holland, 1990
[35] P.L.C. Simon, P.H.S. de Vries and S. Middelhoek, "Autocalibration of silicon hall devices", Sens. Actuators A, Vol. 52, pp. 203-207, 1996
[36] J.M. Dias Pereira, O. Postolache, P. Silva Girão, M. Cretu, "Minimising temperature drift errors of conditioning circuits using Artificial Neural Networks", IEEE Trans. Instr. Meas., Vol.49, No,5, October 2000
[37] J.M. Dias Pereira, O. Postolache, P. Silva Girão, J.A. Brandão Faria, M. Cretu, "An optical temperature transducer based on a bimetallic sensor", 10th International Symposium on Development in Digital Measuring Instrumentation (ISDDMI'98), Vol.2, pp. 661-664, Nápoles, Itália, September 1998
[38] O. Postolache, P. Silva Girão, J.M. Dias Pereira, "Neural Network Application in a carbon monoxide measurement system", IJCNN'01, Washington DC. USA, 2001.
[39] O. Postolache, J.M. Dias Pereira, P. Silva Girão, M. Cretu, "A virtual magnetometer based on Artificial Neural Networks", 10th International Symposium on Development in Digital Measuring Instrumentation (ISDDMI'98), Vol.2, pp. 580-584, Naples, Italy, September 1998.
[40] O. Postolache, J.M. Dias Pereira, M. Cretu, P. Silva Girão, "An ANN Fault Detection procedure applied in virtual measurement systems case", Proc. of IMTC/98", Vol. 1, pp. 257-260, St. Paul, Minnesota, USA, May 1998

[41] J. Patra, A. Kot, G. Panda, "An intelligent pressure sensor using Neural Netwoks", IEEE Trans. Instr. Meas., Vol. 49, No. 4, pp. 829-834, August 2000

[42] J. Pereira, O. Postolache, P. Girão, "A temperature-compensated system for magnetic field measurements based on Artificial Neural Networks", IEEE Trans. Instr. Meas., Vol 47, No.2., pp.494-498, April 1998

[43] M.T. Hagan and M.B. Menhaj, "Training feedforward networks with the Marquardt Algorithm", IEEE Trans. Neural Networks, Vol. 5, No. 6, pp. 989-993, 1994

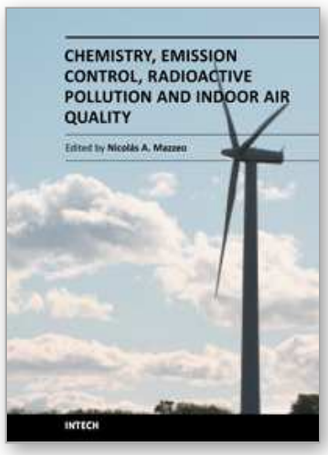

Chemistry, Emission Control, Radioactive Pollution and Indoor Air Quality

Edited by Dr. Nicolas Mazzeo

ISBN 978-953-307-316-3
Hard cover, 680 pages
Publisher InTech
Published online 27, July, 2011
Published in print edition July, 2011

The atmosphere may be our most precious resource. Accordingly, the balance between its use and protection is a high priority for our civilization. While many of us would consider air pollution to be an issue that the modern world has resolved to a greater extent, it still appears to have considerable influence on the global environment. In many countries with ambitious economic growth targets the acceptable levels of air pollution have been transgressed. Serious respiratory disease related problems have been identified with both indoor and outdoor pollution throughout the world. The 25 chapters of this book deal with several air pollution issues grouped into the following sections: a) air pollution chemistry; b) air pollutant emission control; c) radioactive pollution and d) indoor air quality.

INTECH
open science | open minds

InTech Europe
University Campus STeP Ri
Slavka Krautzeka 83/A
51000 Rijeka, Croatia
Phone: +385 (51) 770 447
Fax: +385 (51) 686 166
www.intechopen.com

InTech China
Unit 405, Office Block, Hotel Equatorial Shanghai
No.65, Yan An Road (West), Shanghai, 200040, China
中国上海市延安西路65号上海国际贵都大饭店办公楼405单元
Phone: +86-21-62489820
Fax: +86-21-62489821

IntechOpen